

This is the accepted manuscript made available via CHORUS. The article has been published as:

Multiple scaling power in liquid gallium under pressure conditions

Renfeng Li, Luhong Wang, Liangliang Li, Tony Yu, Haiyan Zhao, Karena W. Chapman, Mark L. Rivers, Peter J. Chupas, Ho-kwang Mao, and Haozhe Liu

Phys. Rev. B **95**, 224204 — Published 6 June 2017

DOI: [10.1103/PhysRevB.95.224204](https://doi.org/10.1103/PhysRevB.95.224204)

1 **The multiple scaling power in liquid gallium under pressure conditions**

2 Renfeng Li,^{1,2} Luhong Wang^{1,*}, Liangliang Li,^{1,2,3} Tony Yu,⁴ Haiyan Zhao,^{3,5} Karena W. Chapman,³
3 Mark L. Rivers,⁴ Peter J. Chupas,³ Ho-kwang Mao^{2,6} and Haozhe Liu^{2,1,*}

4

5 ¹*Harbin Institute of Technology, Harbin 150080, China*

6 ²*Center for High Pressure Science and Technology Advanced Research, Changchun 130015 &*
7 *Beijing 100094, China*

8 ³*Advanced Photon Source, Argonne National Laboratory, Argonne, Illinois 60439, USA*

9 ⁴*Center for Advanced Radiation Sources, The University of Chicago, Chicago, Illinois 60637, USA*

10 ⁵*Center for Advanced Energy Studies, University of Idaho, Idaho Falls, Idaho 83406, USA*

11 ⁶*Geophysical Laboratory, Carnegie Institution, Washington DC 20015, USA*

12

13 Generally, a single scaling exponent, D_f , can characterize the fractal structures of metallic
14 glasses according to the scaling power law. However, when the scaling power law is
15 applied to liquid gallium upon compression, the results show multiple scaling exponents
16 and the values are beyond 3 within the first four coordination spheres in real space,
17 indicating that the power law fails to describe the fractal feature in liquid gallium. The
18 increase in the first coordination number with pressure leads to that first coordination
19 spheres at different pressures are not similar to each other in geometrical sense. This
20 multiple scaling power behavior is confined within a correlation length of $\xi \approx 14\text{-}15 \text{ \AA}$ at
21 applied pressure according to decay of $G(r)$ in liquid gallium. Beyond this length the
22 liquid gallium system could roughly be viewed as homogeneous, as indicated by that the
23 scaling exponent, D_s , is close to 3 beyond the first four coordination spheres.

1 In nature, many shapes exhibit fractal structures, such as clouds, trees, mountains, rivers,
2 coastlines and so on. The existence of these fractal structures originates from the presence
3 of disorder.¹ Consequently, it is accepted that fractal structures spread into disordered
4 condensed matter systems, such as glass and liquid systems. Recently, D. Ma *et al.* linked
5 the structure of metallic glasses to the fractal network and discovered that metallic glasses
6 have fractal characteristics within the medium-range length scale, as indicated by the 2.31
7 power law scaling of the first peak position of the structure factor with the atomic
8 volume.² Subsequently, non-integral 2.5 power law scaling was discovered in metallic
9 glasses under pressure conditions, not only in reciprocal space but also in real space, and
10 it extended beyond the first peak, depending on the specific system.³⁻⁵⁶ Any non-integral
11 power corresponds to a fractal dimensionality, D_f .⁷ Thus, the volume dependence of the
12 first peak position for liquid alkali metals in both real and reciprocal space follows the 3
13 power law under compressed conditions, indicating that liquid alkali metals systems are
14 homogeneous and hence the corresponding D_f is equivalent to the Euclidean dimension,
15 D_e .^{8,9} In metallic glasses and liquid alkali metal systems, a single scaling exponent, D_f ,
16 characterizes the fractal structure of the object.

17
18 Due to the coexistence of metallic and covalent bonding, gallium, a rich polymorphism
19 metal, exhibits unusual and unique physical properties.¹⁰⁻¹⁵ It has a low melting
20 temperature (303 K) and a high boiling temperature (2478 K) at ambient pressure,
21 displaying a wide stability range.¹⁶ At ambient pressure, the density of liquid gallium

1 exceeds that of its stable solid state by approximately 3%, and this liquid metal is easily
2 supercooled.^{17,18} The complex structure of the liquid gallium system under pressure
3 conditions has been studied for many years.^{19,20} However, investigations into its fractal
4 feature under pressure are rare, and hence it is not yet well understood. A little over a
5 decade ago, it was demonstrated that the volume dependence of the first peak position of
6 the pair distribution function (PDF) $g(r)$ for liquid gallium deviating from the 3 power
7 law.⁹ Recently, O. F. Yagafarov *et al.* reported that the scaling of the first four peak
8 positions of $g(r)$ with the atomic volume under pressure conditions presents different
9 values in the liquid state.²¹ Thus, an interesting question has been raised: Could these
10 scaling exponents describe the fractal structure of liquid gallium? In this work, we
11 present the multiple scaling power behavior of liquid gallium and investigate whether
12 fractal behavior exists in liquid gallium.

13
14 High-energy total X-ray scattering data of liquid gallium under pressure at ambient
15 temperature were collected at the 11-ID-B beamline at the Advanced Photon Source,
16 Argonne National Laboratory, with an energy of 86.7 keV. A solid gallium sample with
17 99.9999% purity was heated to a liquid state and then loaded into a T301 stainless steel
18 gasket with a hole as the sample chamber. The supercooled liquid gallium sample was
19 compressed up to 1.9 GPa using a diamond anvil cell, and a ruby ball was used as a
20 pressure marker²².

21
22 Raw image data were reduced using the software FIT-2D²³ with masking strategy²⁴ to

1 remove the diamond peaks to obtain one-dimensional scattering data. The reduced PDF
 2 $G(r)$ and structure factor $S(Q)$ were extracted using the PDFGETX2 program²⁵ after
 3 subtracting contributions from the sample environment and background, and the program
 4 performed a numerical Fourier transform of $S(Q)$ according to

$$5 \quad G(r) = 4\pi r \rho_0 (g(r) - 1) = \frac{2}{\pi} \int_0^\infty Q [S(Q) - 1] \sin(Qr) dQ, \quad (1)$$

6 where ρ_0 is the average atomic number density, and $g(r)$ is the PDF. The average atomic
 7 number density as a function of the pressure at ambient temperature was based on X-ray
 8 microtomography measurements in which the isothermal bulk modulus was determined
 9 to be $B_0 = 23.6$ GPa. The experimental method used to obtain the volume measurements
 10 was described in detail in our previous study.²⁶

11

12 The structure factor $S(Q)$ and the corresponding PDFs under various pressure conditions
 13 are shown in Fig. 1. In real space, the $G(r)$ of liquid gallium oscillates above and below
 14 zero, and the amplitude falls off rapidly with increasing r . These oscillations provide
 15 information regarding the correlations of atomic pairs and suggest a heterogeneous
 16 density in the system according to the atomic PDFs, $\rho(r) = \rho_0 g(r)$. This heterogeneous
 17 distribution of density and the decay of the PDFs in real space may correspond to a
 18 fractal structure in liquid gallium, displaying self-similarity and scale invariance.^{2,27} In a
 19 physical system, the self-similarity and scale invariance are limited to a finite range
 20 between upper and lower bounds. The lower scale is not less than the shortest distance
 21 between two atoms in the system. The upper scale depends on the correlation length

according to the percolation model. The correlation length ξ is the mean radius of the
 gyration of all the finite clusters. This length gives an idea of the average distance at
 which the connectivity makes itself felt. For any length scale $r > \xi$, a percolating system
 is macroscopically homogeneous. Whereas, for $r < \xi$, the system is not homogeneous. In
 this regime, the sample-spanning cluster is self-similar on average.²⁸ Suppose the site
 correspond in some sense to gallium atoms of three-dimensional network. The sites are
 occupied when probability of finding two atoms is non-zero according to $G(r)$. In contrast,
 the non-occupied sites are in opposite situation. The percolation transition is caused by
 variation of the occupancy of the sites or bonds leading to the appearance of the infinite
 cluster at the percolation threshold p_c . At each pressure conditions, there is no parameter
 changes and hence the probability of occupancy is unchanged. Thus, the liquid gallium
 system can be viewed as a system that already formed infinite cluster for consideration of
 dense packed atomic structure of liquid gallium. In other words, the concentration p is
 over percolation threshold p_c already. Since correlation length is finite above p_c , the
 infinite cluster can be self-similar only on length scales smaller than correlation length.
 For length scales larger than correlation length, the structure is not self-similar and can be
 considered as homogeneous.^{29,30} This correlation length can be estimated as $\xi \approx 14\text{-}15\text{\AA}$
 at all pressures according to the decay of $G(r)$ in liquid gallium, as shown in the Fig. 1
 (b).

1 Within the limitation of the correlation lengths, the structural unit clusters that constitute
 2 the liquid gallium system are self-similar and have scale invariance. Thus, the mass of a
 3 cluster increases with its linear dimension r according to the relation

$$4 \quad M(r) \propto r^{D_f},^{31} \quad (2)$$

5 where D_f is the fractal dimensionality. To determine D_f , a common method was employed.
 6 This method consists of covering the object in D_f dimension with boxes whose volumes
 7 are taken as the unit of measurement. If ε is the side of the box, and N is the number of
 8 boxes, then the volume of the object is

$$9 \quad V_0 = N \times \varepsilon^{D_f}.^{32} \quad (3)$$

10 The D_f dimension is determined by

$$11 \quad D_f = \log N / \log(1/\varepsilon).^{33} \quad (4)$$

12 To assume that the compression is uniform in each direction, Eq. (3) under compressed
 13 conditions can be written as

$$14 \quad V_P = N \times \varepsilon_P^{D_f}, \quad (5)$$

15 where V_P is the volume, and ε_P is the counterpart of ε under pressure conditions.

16 According to Eqs. (3) and (5), we have

$$17 \quad V_P/V_0 = (\varepsilon_P/\varepsilon)^{D_f}. \quad (6)$$

18 To link the structure of the object to the fractal dimension, let the length r_i be the side of a
 19 unit box covering the object, where r_i is the peak position of the PDFs in real space. Then,
 20 the scaling law in Eq. (6) is expressed as

$$V_P/V_0 = (r_{iP}/r_{i0})^{D_f} \quad (7)$$

Fractal dimensionality D_f is a universal parameter, thus, the D_f extracted from real space and reciprocal space is equivalent. By analogy to Eq. (7) in real space, we have

$$V_P/V_0 = \left(Q_{i0}/Q_{iP} \right)^{D_f} \quad (8)$$

where Q_i is the peak position of the structure factor. The scaling power law Eqs. (7) and (8) are consistent with the results of previous studies of metallic glasses under pressure.³⁻⁵

According to the same volume compression rate and D_f in Eqs. (7) and (8), the Q_i should be correlated to a distance in real space. If A is a converted factor of the distance for Q_i from the reciprocal space to the real space, then $2\pi A/Q_i$ is the side of the covering unit box. The data points in PDF curves and structure factor $S(Q)$ raw curves could be transformed through Eq. (1).

Whether the scaling power law is suitable for liquid gallium and whether the scaling power is a fractal dimensionality remain unclear. Thus, before the determination, D_s represented the scaling power, and D_f was the fractal dimensionality. In an experimental $S(Q)$, the range of Q is finite; as a result, termination ripples in $G(r)$ appear in the Fourier transformation. These ripples have an effect on the peak position of $G(r)$, which further affects the value of the scaling power D_s according to Eq. (7). However, termination ripples are not a real issue if data are measured to sufficiently high Q_{max} values as the signal in the real $S(Q)$ dies off because of the Debye-Waller factor.³⁴ For liquid gallium,

1 the signal of $S(Q)$ almost dies off, and $S(Q)$ converges to unity at ca. $Q = 11 \text{ \AA}^{-1}$ (inset of
2 Fig. 2) in the measured data. Thus, the Q_{max} in this study is high enough that termination
3 ripples have little effect on the peak position of $G(r)$. Figure 2 shows the $G(r)$ of liquid
4 gallium obtained from Fourier transforming the experimental $S(Q)$ terminated at two
5 selected $Q_{max} = 11 \text{ \AA}^{-1}$ and $Q_{max} = 12 \text{ \AA}^{-1}$ under selected pressure conditions. Clearly,
6 these two set of peak positions in $G(r)$ are essentially the same, hence, the value of the
7 scaling exponent D_s for liquid gallium determined in this work is precise.

8

9 To examine the fractal behavior of liquid gallium in real space and reciprocal space, we
10 applied Eqs. (7) and (8) to the liquid gallium system under compressed conditions and
11 selected r_i and $2\pi A/Q_i$ as the units of measurement, respectively. The volume as a
12 function of pressure was determined using X-ray microtomography measurements, as
13 presented in the inset of Fig. 1 (a). In real space, the relation between V_P/V_0 and r_{iP}/r_{i0} ($i >$
14 7) becomes featureless and could not be fitted because of the decay of the PDFs, whereas
15 the featured volume scaling relations were limited within Q_2 in reciprocal space. The
16 fitting results are shown in Fig. 3, in which scaling of both r_{iP}/r_{i0} and Q_{i0}/Q_{iP} with V_P/V_0
17 present multiple exponents. This phenomenon is consistent with previous study in which
18 r_{iP}/r_{i0} ($i = 1-4$) was scaled by density for the first four coordination spheres.²¹ The
19 non-cubic scaling of r_I was also reported in liquid metal Bi.⁹ The D_{sr3} , D_{sr4} and D_{sQI} are
20 approximately equal, indicating that the length corresponding to Q_I is between r_3 and r_4 .
21 This result suggests that Q_I indeed embodied a medium-range order. Likewise, the value

1 of D_{sQ2} was close to that of D_{sr1} and far from that of D_{sr2} , indicating that Q_2 indeed
 2 embodied the information of short-range order. Again, these results suggest that the
 3 scaling power determined by the real and reciprocal space are equivalent, as described
 4 above. Therefore, the following discussion will focus on the real space to simplify the
 5 argument.

6

7 In conventional single scaling, D_f is independent of the measurement unit; for example,
 8 $D_f = 2.5$ is almost constant in metallic glass systems under pressure. However, in the
 9 liquid gallium system, D_s is a function of the measurement unit and decreases with the
 10 linear dimension r . Although mathematically the exponent D_s in power law fitting could
 11 be any real number which loosely links to Hausdorff dimensionality, it is generally
 12 accepted an inequality $D_f < D_e$ for the fractal dimensionality. Hence the scaling exponent
 13 exceeding 3 within the first coordination sphere directly indicates that the scaling power
 14 fails to describe the fractal feature in liquid gallium. To find out the reason for this failure,
 15 we examined the changes of the atom number within the first coordination sphere with
 16 pressure increased.

17

18 The first coordination number (CN) at various pressures was calculated by

$$19 \quad CN = \int_{r_1}^{r_2} R(r) dr, \quad (9)$$

20 where $R(r) = 4\pi r^2 \rho(r)$ is the radial distribution function (RDF), and r_1 and r_2 define the
 21 beginning and ending positions, respectively, of the RDF peak corresponding to the

1 coordination shell, as shown in Fig. 4 (inset). The limits of the left side of the first peak r_1
 2 can be easily determined. However, despite reducing the ripples in the RDF, the limits of
 3 the right side of the first peak r_2 may fluctuate because of the contributions from different
 4 errors. The first CN is sensitive to these fluctuations, thus the value of r_2 was averaged
 5 for all curves at various pressures²¹ for consideration of the minor changes in the first
 6 peak position and the low applied pressure in this work. Defined $r_1 = 2.3 \text{ \AA}$ and $r_2 = 3.71$
 7 \AA , the first CN as a function of the pressure is presented in Fig. 4, which displays that the
 8 value of CN for liquid gallium increases gradually from 11.4 to 12.1 as the pressure
 9 increases from 0 to 1.9 GPa. Previous studies on liquid gallium also reported an increase
 10 in the first CN with pressure.^{20,21,35-37} This automatically indicates the first coordination
 11 spheres are not similar to each other at various pressure conditions in geometrical sense,
 12 since the increased first coordination number means more atoms move into the nearest
 13 neighbor shell. The scaling power of r_1 with a volume in liquid gallium is quite close to a
 14 constant and above 3, which is consequence of the increased first coordination number.
 15 The multiple scaling power for the first four peaks might result from different paces of
 16 decrease in various coordination spheres. Thus, the scaling power law in Eqs. (7) and (8)
 17 cannot be used to obtain the fractal dimensionality for liquid gallium under pressure,
 18 considering a prerequisite for both equations is that the fractal dimensionality is constant
 19 under pressure.

20

1 The fractal feature relates to the nonuniformity of the density in physical systems. In
2 crystalline metal or alloy systems, the density is uniform and a fractal feature is absent,
3 thus the fractal dimensionalities $D_f = D_e = 3$ match the scaling power of 3. For liquid
4 gallium, although the scaling power law fails to describe the fractal feature, fractal
5 behavior may exist because the fitting results show that D_{sr5} , D_{sr6} and D_{sr7} are close to 3.
6 It indicates that beyond the length scale of r_5 , the system could be viewed as
7 homogeneous and the fractal feature disappears, which is consistent with the range
8 confined by the correlation length. Notably, the fractal dimensionality is independent of
9 the pressure when the density is homogeneous ($D_f = D_e = 3$), and hence examining the
10 homogeneous feature in liquid gallium according to Eq. (8) is appropriate.

11

12 The multiple scaling power behavior illustrates that decreases in the volume and atomic
13 distance follow the scaling power, despite its failure to describe the fractal feature in
14 liquid gallium. This implies that the structural evolution in liquid gallium under pressure
15 likely obeys a general rule of multiple scaling power. Furthermore, the multiple scaling
16 power behavior in liquid gallium provides information on the contraction of the atomic
17 distance r_i ($i < 8$) or various coordination spheres under pressure. The greater the power
18 D_s , the less contracted the coordination spheres should be. The $D_{sr1}=11.2(3)$ is far greater
19 than D_{sri} ($1 < i < 8$), namely, the rate of decrease in the first nearest coordination sphere is
20 slower than those of other coordination spheres, suggesting that the decrease in the
21 volume of liquid gallium under pressure can be mainly attributed to the shrinkage of

1 other further coordination spheres. Moreover, the $D_{srl}=11.2(3)$ embodies a moderate
2 decrease in the first nearest coordination sphere, which is correlated to an increase in the
3 first CN under compressed conditions.^{20,21}

4
5 In summary, although the scaling power law fails to describe the fractal behavior in liquid
6 gallium under pressure, it provides important information on the changes of coordination
7 sphere. Furthermore, based on the percolation model, fractal behavior is suggested in
8 liquid gallium within a limited correlation length of $\xi \approx 14-15$ Å. The multiple scaling
9 power behavior observed in liquid gallium is supplementary to a previous discovery of
10 single fractal dimensionality in metallic glass systems. We hope that our study could
11 advance the research on fractal in the broad field of disordered condensed matter systems.

12
13 This work was performed at Argonne National Laboratory and use of the Advanced
14 Photon Source was supported by the US Department of Energy, Office of Science, Office
15 of Basic Energy Sciences, under contract No. DE-AC02-06CH11357. GSECARS is
16 supported by the National Science Foundation (NSF)-Earth Sciences (EAR-1128799) and
17 Department of Energy (DoE)-GeoSciences (DE-FG02-94ER14466). This work was
18 supported by the National Natural Science Foundation of China (U1530402, 11374075),
19 Heilongjiang Province Science Fund for Distinguished Young Scholars (JC201005),
20 Longjiang Scholar, the Fundamental Research Funds for the Central Universities (HIT.
21 BRET1.2010002, HIT. IBRSEM.A.201403), HIT-Argonne Overseas Collaborative Base

1 Project, and Chinese Scholarship Council. This work acknowledges US NSF support
2 EAR-1620548.

3

4

¹ B. B. Mandelbrot, *The Fractal Geometry of Nature* (Updated and Augmented Edition)
(W. H. Freeman, New York, 1983), Chap. 1, p. 18.

² D. Ma, A. D. Stoica, and X. L. Wang, *Nature Mater.* **8**, 30 (2009).

³ Q. Zeng, Y. Lin, Y. Liu, Z. Zeng, C. Y. Shi, B. Zhang, H. Lou, S. V. Sinogeikin, Y.
Kono, C. Kenney-Benson, C. Park, W. Yang, W. Wang, H. Sheng, H-k. Mao, and W. L.
Mao, *Proc. Natl. Acad. Sci.* **113**, 1714 (2016).

⁴ Q. Zeng, Y. Kono, Y. Lin, Z. Zeng, J. Wang, S. V. Sinogeikin, C. Park, Y. Meng, W.
Yang, H. K. Mao, and W. L. Mao, *Phys. Rev. Lett.* **112**, 185502 (2014).

⁵ D. Z. Chen, C. Y. Shi, Q. An, Q. Zeng, W. L. Mao, W. A. Goddard, and J. R. Greer,
Science **349**, 1306 (2015).

⁶ L. Li, L. Wang, R. Li, H. Zhao, D. Qu, K. W. Chapman, P. J. Chupas, and H. Liu,
Phys. Rev. B **94**, 184201 (2016).

⁷ B. B. Mandelbrot, *The Fractal Geometry of Nature* (Updated and Augmented Edition)
(W. H. Freeman, New York, 1983), Chap. 1, p. 15.

⁸ Y. Morimoto, S. Kato, N. Toda, Y. Katayama, K. Tsuji, K. Yaoita, and O. Shimomura,
Rev. High Pressure Sci. Technol. **7**, 245 (1998).

⁹ Y. Katayama and K. Tsuji, *J. Phys.: Condens. Matter* **15**, 6085 (2003).

- ¹⁰ O. Degtyareva, M. I. McMahon, D. R. Allan, and R. J. Nelves, Phys. Rev. Lett. **93**, 205502 (2004).
- ¹¹ Z. Q. Li and J. S. Tse, Phys. Rev. B **62**, 9900 (2000).
- ¹² X. G. Gong, G. L. Chiarotti, M. Parrinello, and E. Tosatti, Phys. Rev. B **43**, 14277 (1991).
- ¹³ O. Züger and U. Dürig, Phys. Rev. B **46**, 7319 (1992).
- ¹⁴ D. A. Walko, I. K. Robinson, C. Grütter, and J. H. Bilgram, Phys. Rev. Lett. **81**, 626 (1998).
- ¹⁵ M. Bernasconi, G. L. Chiarotti, and E. Tosatti, Phys. Rev. B **52**, 9988 (1995).
- ¹⁶ E. L. Gromnitskaya, O. F. Yagafarov, O. V. Stalgorova, V. V. Brazhkin, and A. G. Lyapin, Phys. Rev. Lett. **98**, 165503 (2007).
- ¹⁷ L. Comez, A. Di Cicco, J. P. Itie, and A. Polian, Phys. Rev. B **65**, 014114 (2001).
- ¹⁸ R. Poloni, S. De Panfilis, A. Di Cicco, G. Pratesi, E. Principi, A. Trapananti, and A. Filipponi, Phys. Rev. B **71**, 184111 (2005).
- ¹⁹ P. Ascarelli, Phys. Rev. **143**, 36 (1966).
- ²⁰ T. Yu, J. Chen, L. Ehm, S. Huang, Q. Guo, S. N. Luo, and J. Parise, J. Appl. Phys. **111**, 112629 (2012).
- ²¹ O. F. Yagafarov, Y. Katayama, V. V. Brazhkin, A. G. Lyapin, and H. Saitoh, Phys. Rev. B **86**, 174103 (2012).
- ²² H. K. Mao, J. Xu and P. M. Bell, J. Geophys. Res. **91**, 4673 (1986).
- ²³ A. P. Hammersley, J. Appl. Cryst. **49**, 646 (2016).
- ²⁴ K. W. Chapman *et al.*, J. Appl. Cryst. **43**, 297 (2010).
- ²⁵ X. Qiu, J. W. Thompson and S. J. L. Billinge, J. Appl. Cryst. **37**, 678 (2004).

- ²⁶ R. Li, L. Li, T. Yu, L. Wang, J. Chen, Y. Wang, Z. Cai, J. Chen, M. L. Rivers, and H. Liu, Appl. Phys. Lett. **105**, 041906 (2014).
- ²⁷ L. Börjesson, R. L. McGreew, and W. S. Howells, Philos. Mag. B, **65**, 261 (1992).
- ²⁸ M. Sahimi, *Applications of Percolation Theory* (Taylor & Francis Bristol, PA, 1994), Chap. 2, p. 16.
- ²⁹ A. A. Saberi Phys. Rep. **578**, 1 (2015).
- ³⁰ A. Bunde and S. Havlin, Fractals and Disordered Systems (Second Revised and Enlarged Edition) (Springer, 1996), Chap 2, p. 66.
- ³¹ T. Freltoft, J. K. Kjems and S. K. Sinha, Phys. Rev. B **33**, 269, (1986).
- ³² J.-F. Gouyet, *Physics and Fractal Structures* (Springer, 1996), Chap 1, p. 5.
- ³³ B. B. Mandelbrot, *The Fractal Geometry of Nature* (Updated and Augmented Edition) (W. H. Freeman, New York, 1983), Chap. 2, p. 37.
- ³⁴ T. Egami and S. J. L. Billinge, *Underneath the Bragg Peaks: Structural Analysis of Complex Materials* (Pergamon, 2003), Chap 3, p. 65.
- ³⁵ K. Tsuji, J. Non-Cryst. Solids **117-118**, 27 (1990).
- ³⁶ J. Yang, J. S. Tse, and T. Iitaka, J. Chem. Phys. **135**, 044507 (2011).
- ³⁷ O. F. Yagafarov, Y. Katayama, V. V. Brazhkin, A. G. Lyapin, and H. Saitoh, High Pressure Res. **33**, 191 (2013).

Captions

Fig. 1. (a) Structure factor $S(Q)$ and (b) reduced PDFs $G(r)$ of liquid gallium at various pressure conditions. The inset of (a) shows the reconstructed 3D images from X-ray microtomography measurements on the volumes under the applied pressures.

Fig. 2. $G(r)$ of liquid gallium obtained from Fourier transforming the experimental $S(Q)$ terminated at $Q_{max} = 11 \text{ \AA}^{-1}$ (indicated by arrow) and $Q_{max} = 12 \text{ \AA}^{-1}$ under 1.0 GPa. The inset corresponds to the experimental $S(Q)$.

Fig. 3. The relative volume V_P/V_0 scaling with (a) the ratio of the i^{th} peak position r_i in real space, where $i = 1, 2, 3, 4, 5, 6$ and 7 , and (b) the ratio of the first and second peak positions in reciprocal space.

Fig. 4. The first CN as a function of the pressure in liquid gallium. The inset shows the definition of the area under the first peak.

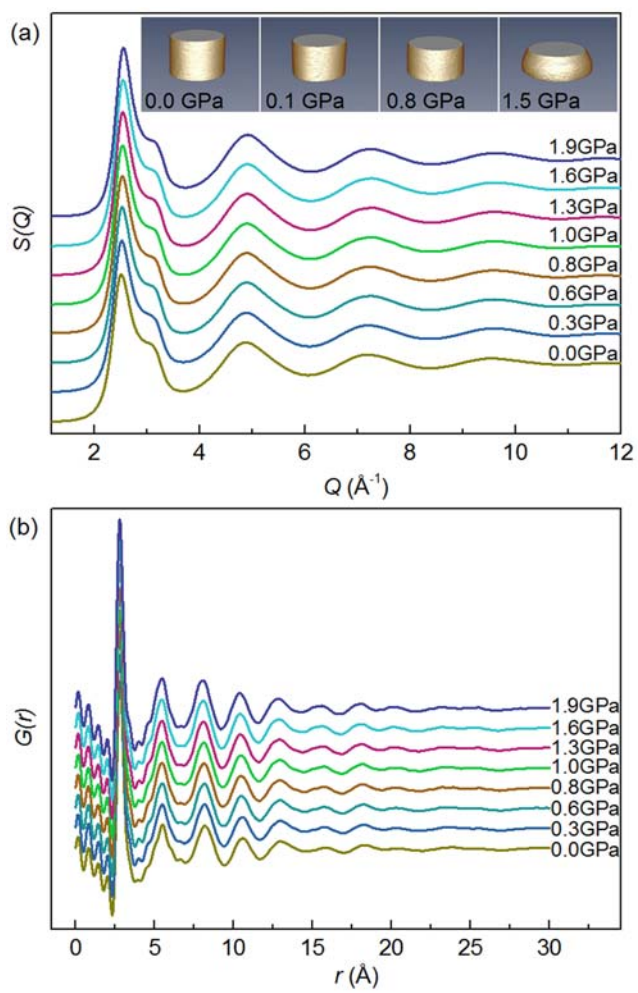


Fig. 1.

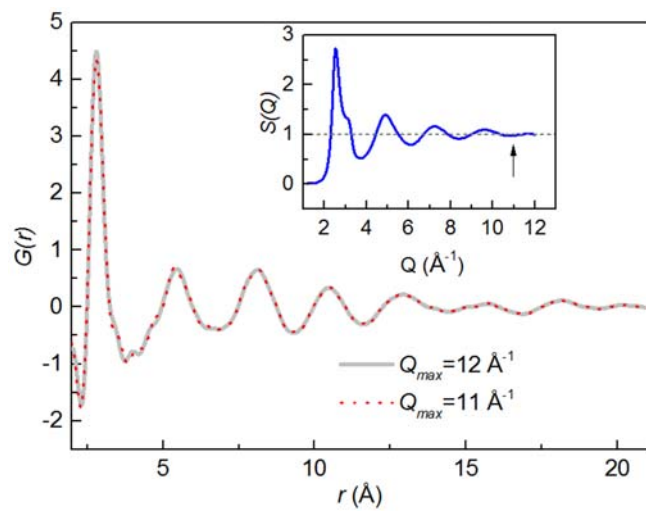


Fig. 2.

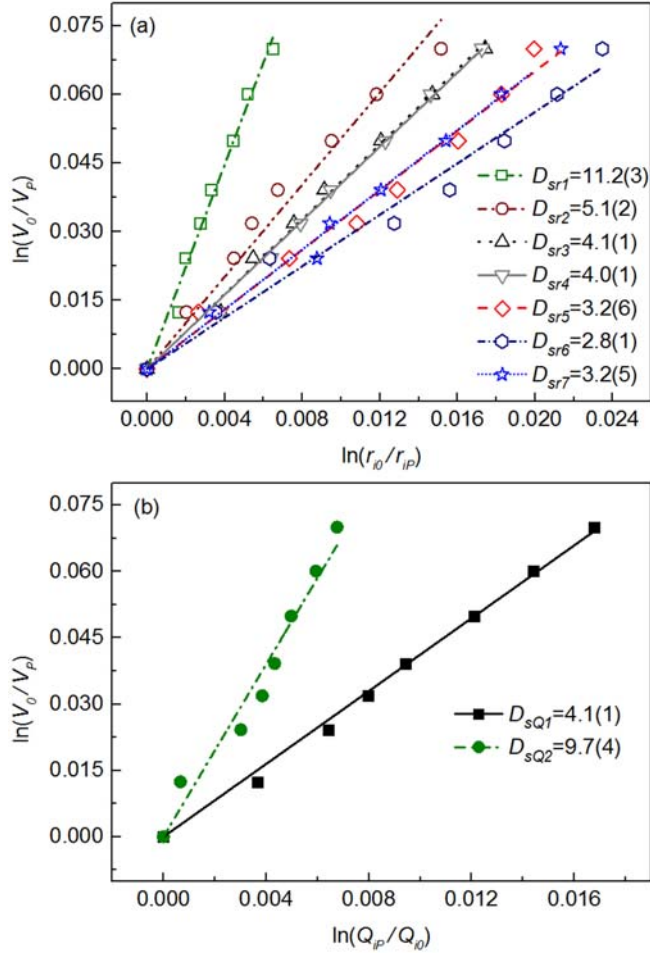


Fig. 3.

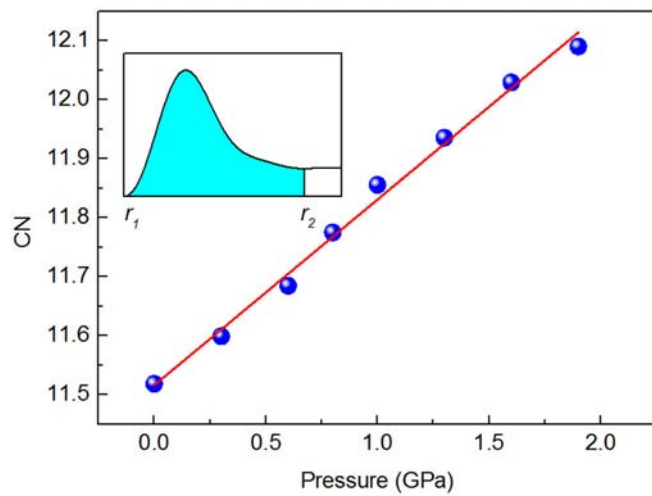


Fig. 4.